

UCLA

UCLA Previously Published Works

Title

Human developmental chondrogenesis as a basis for engineering chondrocytes from pluripotent stem cells.

Permalink

<https://escholarship.org/uc/item/60c1v43t>

Journal

Stem Cell Reports, 1(6)

ISSN

2213-6711

Authors

Wu, Ling

Bluguermann, Carolina

Kyupelyan, Levon

et al.

Publication Date

2013

DOI

10.1016/j.stemcr.2013.10.012

Copyright Information

This work is made available under the terms of a Creative Commons Attribution-NonCommercial-NoDerivatives License, available at

<https://creativecommons.org/licenses/by-nc-nd/4.0/>

Peer reviewed

Human Developmental Chondrogenesis as a Basis for Engineering Chondrocytes from Pluripotent Stem Cells

Ling Wu,^{1,9} Carolina Bluguermann,^{1,8,9} Levon Kyupelyan,¹ Brooke Latour,² Stephanie Gonzalez,¹ Saumya Shah,¹ Zoran Galic,³ Sundi Ge,² Yuhua Zhu,² Frank A. Petrigliano,¹ Ali Nsair,^{3,7} Santiago G. Miriuka,⁸ Xinmin Li,² Karen M. Lyons,^{1,6} Gay M. Crooks,^{2,3,5} David R. McAllister,¹ Ben Van Handel,⁴ John S. Adams,^{1,3,5} and Denis Evseenko^{1,3,5,*}

¹Department of Orthopaedic Surgery, Orthopedic Hospital Research Center, David Geffen School of Medicine, University of California at Los Angeles, Los Angeles, CA 90095, USA

²Department of Pathology and Laboratory Medicine, David Geffen School of Medicine, University of California at Los Angeles, Los Angeles, CA 90095, USA

³Broad Stem Cell Research Center, University of California at Los Angeles, Los Angeles, CA 90095, USA

⁴Novogenix Laboratories, LLC, Los Angeles, CA 90033, USA

⁵Jonsson Comprehensive Cancer Center, University of California at Los Angeles, Los Angeles, CA 90095, USA

⁶Department of Molecular, Cell and Developmental Biology, University of California at Los Angeles, Los Angeles, CA 90095, USA

⁷Department of Medicine and Physiology, Cardiovascular Research Laboratory, David Geffen School of Medicine, University of California at Los Angeles, Los Angeles, CA 90095, USA

⁸Laboratorio de Biología del Desarrollo Celular, Laboratorios de Investigación Aplicada en Neurociencias, Fundación para la Lucha contra las Enfermedades Neurológicas de la Infancia, Escobar B1625XAF, Buenos Aires, Argentina

⁹These authors contributed equally to this work

*Correspondence: devseenko@mednet.ucla.edu
<http://dx.doi.org/10.1016/j.stemcr.2013.10.012>

This is an open-access article distributed under the terms of the Creative Commons Attribution-NonCommercial-No Derivative Works License, which permits non-commercial use, distribution, and reproduction in any medium, provided the original author and source are credited.

SUMMARY

Joint injury and osteoarthritis affect millions of people worldwide, but attempts to generate articular cartilage using adult stem/progenitor cells have been unsuccessful. We hypothesized that recapitulation of the human developmental chondrogenic program using pluripotent stem cells (PSCs) may represent a superior approach for cartilage restoration. Using laser-capture microdissection followed by microarray analysis, we first defined a surface phenotype (CD166^{low/neg}CD146^{low/neg}CD73⁺CD44^{low}BMPR1B⁺) distinguishing the earliest cartilage committed cells (prechondrocytes) at 5–6 weeks of development. Functional studies confirmed these cells are chondrocyte progenitors. From 12 weeks, only the superficial layers of articular cartilage were enriched in cells with this progenitor phenotype. Isolation of cells with a similar immunophenotype from differentiating human PSCs revealed a population of CD166^{low/neg}BMPR1B⁺ putative cartilage-committed progenitors. Taken as a whole, these data define a developmental approach for the generation of highly purified functional human chondrocytes from PSCs that could enable substantial progress in cartilage tissue engineering.

INTRODUCTION

Articular cartilage is a highly specialized tissue formed from chondrocytes that protects the bones of diarthrodial joints from forces associated with load bearing and impact and allows nearly frictionless motion between the articular surfaces (Buckwalter and Mankin, 1998). Cartilage injury and lack of cartilage regeneration often lead to osteoarthritis involving degradation of joints, including articular cartilage and subchondral bone. Osteoarthritis currently affects more than 20 million people in the United States alone, making joint-surface restoration a major priority in modern medicine (Andersson et al., 2011).

Articular chondrocytes are formed during the process of endochondral ossification and joint formation during early embryogenesis (DeLise et al., 2000; Goldring et al., 2006). Different cartilage cell subsets formed during the process of endochondral ossification have been primarily defined based on their morphological appearance. First, the mesenchymal cells of the lateral plate mesoderm condense to

form compact nodules and then differentiate into rapidly dividing prechondrocytes, or transient progenitors, representing the transition of mesenchymal ancestors into chondrocytes (Hall and Miyake, 1995; Woods et al., 2007). Differentiating chondrocytes generated from prechondrocytes continue to divide but also secrete cartilage-specific matrix to form the cartilage template of the bone. There are two major types of chondrocytes generated at this stage: (1) periarticular chondrocytes located in the presumptive joint regions (also known as the interzone) that later will form phenotypically stable or “permanent” articular cartilage (Koyama et al., 2008) and (2) growth plate chondrocytes undergoing proliferation required for bone growth that will eventually express collagen X (*COL10A1*), undergo hypertrophic transformation, and be replaced by bone (Provot and Schipani, 2005). One defining feature of developing articular chondrocytes is their progression through an intermediate expressing growth differentiation factor 5 (GDF5), a ligand for bone morphogenetic protein receptor 1 beta (BMPR1B),



signaling through which is required for cartilage development (Baur et al., 2000; Koyama et al., 2008).

Different cell types have been studied with respect to their ability to generate articular cartilage. However, none of the current cell-based repair strategies, including in-vitro-expanded articular chondrocytes or mesenchymal stem cells (MSCs) from adult bone marrow (BM), adipose tissue, synovium, or amniotic fluid, have generated long-lasting hyaline articular cartilage tissue (Gelse et al., 2008; van Osch et al., 2009). It is not completely clear why adult MSCs from all tested sources fail to generate hyaline articular cartilage. Potentially, the developmental origins of adult MSCs and articular chondrocytes are different. Bona fide cartilage progenitors are likely to be present only early in development. Recapitulation of the human developmental chondrogenic program and generation of chondrocytes from pluripotent stem cells (PSCs) may represent a superior approach for cartilage restoration. Human PSCs have been successfully used by several groups, including ours, to generate cartilage-like tissue (Evseenko et al., 2010; Nakayama et al., 2003; Oldershaw et al., 2010; Toh et al., 2009; Yamashita et al., 2010; Umeda et al., 2012). Some of these published reports involved undifferentiated PSCs as a starting population to make cartilage-like tissue (Oldershaw et al., 2010), while others utilized PSC-derived MSCs as a source for chondrocytes (Nakayama et al., 2003; Umeda et al., 2012). Differentiation of PSCs rarely yields a single cell type, even under optimized conditions, necessitating purification of the cell of interest from other derivatives. None of the previously published studies have reported the generation of a highly purified population of PSC-derived chondrocytes, but rather demonstrated the generation of undefined and unsorted cells with unknown ontogeny capable of depositing chondrogenic matrix molecules. As a result, immunophenotypes and functional characteristics of the earliest cartilage cells derived during differentiation of PSCs are currently not known. To a large extent, this knowledge is missing due to the complete lack of the developmental studies dissecting the earliest stages of human chondrogenesis.

Here, we define the developmental progression through which primordial mesenchymal cells commit to the chondrocyte lineage in vivo. The application of laser-capture microdissection (LCM) and gene expression profiling to human limbs from 5 to 6 weeks of development allowed us to determine candidate cell surface markers and signaling pathways that distinguish the earliest primitive chondrogenic progenitors (prechondrocytes) from other cell types present in the same tissue. Moreover, this phenotype also delineated a subset of cells present in the periarticular region in fetal and adult joints, which evidenced localization and gene expression characteristic of resting (immature) chondrocytes; these data suggest that BMPR1B

distinguishes immature from more differentiated and hypertrophic chondrocytes at fetal and adult stages of human development. Finally, application of this developmentally defined paradigm enabled the directed differentiation of PSCs into immature chondrocytes capable of integrating into fetal joints in vitro and producing matrix. Taken as a whole, these data define a developmental approach for the generation of highly purified functional human chondrocytes from PSCs that could enable substantial progress in cartilage tissue engineering.

RESULTS

Identification of Molecular Markers Distinguishing Prechondrocytes and Other Cell Lineages in Developing Limbs

Chondrogenic development in the proximal regions of the limbs occurs earlier than the distal ones and at 5-6 weeks of human embryogenesis, after the anatomically defined cartilaginous anlagen of long bones such as the humerus has already formed, groups of undifferentiated prechondrocytes remain in distinct sites of the limbs (Figure 1A). Cartilage-committed mesenchymal cells (prechondrocytes) could be identified as nodules with a morphologically “dense” appearance in chondrogenic condensations at weeks 5–6 and minimally stained with cresyl violet, suggesting that they produced little cartilaginous matrix (Figure 1B). Prechondrocytes from 5- to 6-week-old human limbs were isolated using LCM (Figure 1B; N = 6) and subjected to genome-wide expression analysis. To nominate candidate genes that distinguish prechondrocytes from other cell types in the limb at this embryonic stage, RNA was isolated from the same specimens following LCM of prechondrocytes and used for microarray analysis.

Ingenuity Pathway Analysis (IPA) revealed 585 genes significantly differentially expressed in prechondrocytes versus total limb cells, which at this stage includes myoblasts, blood, endothelial cells, keratinocytes, mature chondrocytes, nerves, dermal fibroblasts, and other cell types (Figure 1C; Table 1). Many of the genes enriched in human prechondrocytes (Table 1A; Table S1 available online) were previously found at the initial stages of chondrogenesis in the chick or mouse embryo, indicating the purity of LCM-isolated prechondrocytes. These genes included *SOX5*, *SOX6*, *SOX9*, *NKX 3-2*, *FOXP4*, *GDF5*, *PCDH8* and *PCDH10*, *BMPR1B*, and *PTCH1* (Table 1; Cameron et al., 2009; DeLise et al., 2000; Goldring et al., 2006). In agreement with these data, principal component analysis carried out on total expression data (Figure 1D) demonstrated that all six replicates of prechondrocyte data clustered together and distinctly from total limb cells.

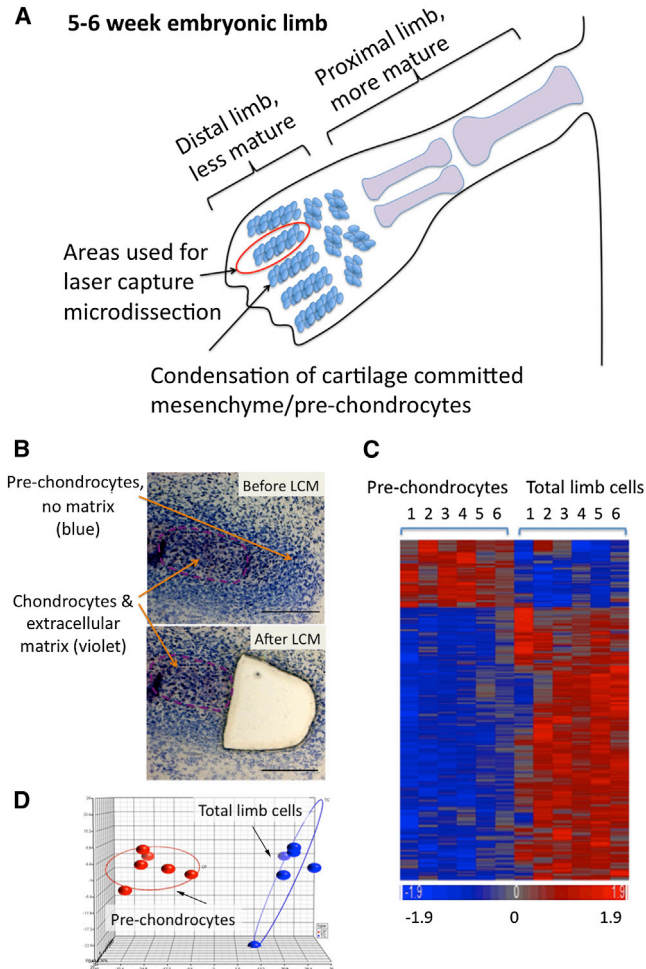


Figure 1. Prechondrocytes Represent a Transcriptionally Distinct Population in Developing Limbs

(A) Schematic representation of chondrocyte commitment and maturation in the early human limb. Light blue spheres represent condensing cartilage-committed mesenchymal cells.

(B) Representative image of chondrogenic regions before and after laser-capture dissection. Sections were prestained with cresyl violet. Scale bar, 100 μ m.

(C) Unsupervised gene cluster analysis of significantly differentially expressed genes in laser-capture microdissected prechondrocytes (PC) from 5- to 6-week specimens versus total limb cells (TLC) from the same specimen.

(D) Principal component analysis demonstrated the reproducibility of data between biological replicates.

See also [Table S1](#).

To interrogate these findings at the cellular level, we performed immunohistochemistry (IHC) to localize commonly used mesenchymal markers and the cell surface markers identified in the microarray study. Expression of these candidates was evaluated on both prechondrocytes ([Figures 2A and 2B](#)) present in the less differentiated

peripheral regions of condensations and the more differentiated chondrocytes present in both the central zones at 6–7 weeks of development ([Figure 2B](#)) as well as long bones in the proximal regions ([Figures 2A and 2C](#)). All analyzed markers could be divided into three groups based on the pattern of antigen expression on prechondrocytes and more mature, matrix-producing chondrocytes. In the first group of tested antigens, low expression levels were found in prechondrocytes (undergoing de novo chondrogenic commitment) located in the periphery of forming condensation and high expression detected in more mature chondrocytes located in the central part of the anlagen. This pattern was detected for CD44 ([Figure 2B](#)) and also for several other molecules including Syndecan 4 (SDC4), FGFR2, and PTCH1 ([Figure S1](#)). The level of CD44 expression was most different between prechondrocytes and more mature chondrocytes. The second group of antigens showed declining expression levels from condensed prechondrocytes to differentiated chondrocytes. This pattern was detected for CD146 and CD166 ([Figure 2B](#)), as well as CD56/neural cell adhesion molecule 1 (NCAM1) and protocadherins (PCDH) 8 and 10 ([Figure S1](#)). The third group of antigens showed no difference in expression between prechondrocytes and mature chondrocytes, including CD73, BMPRI1B (expressed in both cell types at this early stage of development; [Figures 2B and 2C](#)), and CD34 (expressed at low or undetectable levels in both cell types; [Figure S1](#)). CD166 was clearly expressed in the primitive mesenchymal cells surrounding chondrogenic condensations and was significantly downregulated on prechondrocytes and absent on mature chondrocytes. As expected, the vast majority of prechondrocytes were dividing as detected by Ki67 staining ([Figures 2A and 2B](#)). These data confirmed the gene expression data and indicated that separation of prechondrocytes from total limb cells, including more differentiated mature chondrocytes, may be possible with surface markers.

Defining Molecular Landmarks of Prechondrocyte Differentiation and Maturation

We next wanted to identify surface markers that would demarcate definitive resting (immature) periarticular chondrocytes from hypertrophic chondrocytes during their maturation from prechondrocytes. To define molecular markers during the process of prechondrocyte maturation, resting periarticular chondrocytes were dissected from femoral bone epiphysis of 17-week specimens ([Figure 3A](#)) and compared with prechondrocytes dissected with LCM from 5- to 6-week-old specimens. We use the term “resting periarticular chondrocytes” for dissected cells (~ 200 μ m layer) to emphasize that dissected cells were clearly separated from more mature proliferating and hypertrophic chondrocytes in the forming growth plate. Our studies



Table 1. Transcriptional Signatures of Cartilage Cells at Different Stages of Human Development

| Prechondrocytes versus Total Limb Cells at 5–6 Weeks | | | Embryonic Prechondrocytes at 5–6 Weeks versus Immature Resting Fetal Chondrocytes at 17 Weeks | | | | | |
|--|-----------------------|-------------|---|-----------------------|-------------|---------------------------|-----------------------|-------------|
| Gene Symbol | p Value | Fold Change | Gene Symbol | p Value | Fold change | Gene Symbol | p Value | Fold Change |
| Receptors and Adhesion Molecules | | | Receptors and Adhesion Molecules | | | | | |
| <i>OPRK1</i> | 0.00459503 | 5.2 | <i>EPHA7</i> | 3.26×10^{-8} | 113 | <i>ITGA9</i> | 1.78×10^{-7} | -5.4 |
| <i>PCDH10</i> | 0.000751492 | 3.1 | <i>PCDH8</i> | 2.53×10^{-7} | 102.4 | <i>GREM1</i> | 0.00432727 | -6.1 |
| <i>BMPR1B</i> | 0.000134191 | 2.9 | <i>EPHA4</i> | 4.50×10^{-6} | 83.5 | <i>CD59</i> | 1.27×10^{-6} | -6.5 |
| <i>CD44</i> | 0.0151098 | 2.3 | <i>PCDH18</i> | 7.34×10^{-8} | 81.7 | <i>CD82</i> | 1.48×10^{-6} | -6.5 |
| <i>FGFR2</i> | 0.000195311 | 2.2 | <i>OPRK1</i> | 2.49×10^{-7} | 72.8 | <i>CD164</i> | 1.26×10^{-6} | -9.9 |
| <i>FZD9</i> | 0.0148514 | 2.2 | <i>CD24</i> | 3.75×10^{-7} | 58.3 | <i>ITGB3</i> | 9.77×10^{-8} | -11.3 |
| <i>PTCH1</i> | 0.000635444 | 2.2 | <i>CD200</i> | 3.42×10^{-7} | 45.8 | <i>ITGB1</i> | 1.84×10^{-5} | -11.5 |
| <i>ITGA10</i> | 0.0246543 | 2.1 | <i>PCDHB10</i> | 3.86×10^{-7} | 31.6 | <i>ITGA5</i> | 1.08×10^{-8} | -13.8 |
| <i>PCDH8</i> | 0.0396394 | 1.8 | <i>CDH2</i> | 1.81×10^{-7} | 24.4 | <i>CD276</i> | 7.93×10^{-9} | -15.4 |
| <i>FZD8</i> | 0.00291429 | 1.8 | <i>CDH10</i> | 3.65×10^{-7} | 22.3 | <i>LIFR</i> | 1.09×10^{-8} | -17.2 |
| <i>FGFRL1</i> | 0.00167931 | 1.6 | <i>FZD2</i> | 2.34×10^{-8} | 20.4 | <i>CD58</i> | 1.14×10^{-8} | -16.2 |
| <i>SDC4</i> | 0.0224326 | 1.5 | <i>ITGB8</i> | 5.95×10^{-7} | 19.9 | <i>CD55</i> | 2.10×10^{-6} | -18.6 |
| Growth Factors/Morphogens | | | <i>FZD3</i> | 9.66×10^{-6} | 19.2 | <i>CD109</i> | 3.40×10^{-8} | -19.3 |
| <i>GDF5</i> | 0.000129624 | 4.4 | <i>CD146/MCAM</i> | 1.60×10^{-7} | 17.8 | <i>CD46</i> | 1.06×10^{-7} | -24.2 |
| <i>PTH1H</i> | 0.0020495 | 3.8 | <i>IL11RA</i> | 6.48×10^{-7} | 16.7 | <i>CD73/NT5E</i> | 3.81×10^{-7} | -72.4 |
| <i>WNT16</i> | 0.0171712 | 2.6 | <i>FZD4</i> | 1.84×10^{-6} | 14.4 | <i>CD44</i> | 2.37×10^{-7} | -82.7 |
| <i>SCRG1</i> | 0.00548691 | 2.6 | <i>CD248</i> | 2.08×10^{-6} | 12.2 | <i>ICAM1</i> | 1.36×10^{-7} | -181.2 |
| <i>NOG</i> | 0.00513526 | 2.4 | <i>LEPR</i> | 9.95×10^{-6} | 11.9 | Growth Factors/Morphogens | | |
| <i>GDF10</i> | 0.0280791 | 2.2 | <i>BMPR1B</i> | 2.42×10^{-5} | 11.5 | <i>DKK1</i> | 0.000128204 | 42.2 |
| Transcription Factors | | | <i>PCDH7</i> | 1.84×10^{-5} | 10.7 | <i>DKK2</i> | 3.54×10^{-6} | 41.1 |
| <i>FOXC1</i> | 6.99×10^{-7} | 3.4 | <i>CADM1</i> | 1.84×10^{-7} | 10.1 | <i>NOG</i> | 2.07×10^{-5} | 34.2 |
| <i>SOX5</i> | 6.69×10^{-6} | 3.4 | <i>EGFR</i> | 1.58×10^{-5} | 9.6 | <i>FGF13</i> | 2.91×10^{-6} | 27.3 |
| <i>SOX6</i> | 8.27×10^{-6} | 3.3 | <i>GABRB3</i> | 1.71×10^{-6} | 9.4 | <i>FST</i> | 1.77×10^{-6} | 23.6 |
| <i>NKX3.2</i> | 3.91×10^{-5} | 3 | <i>CD56/NCAM1</i> | 7.77×10^{-5} | 9.3 | <i>GDF10</i> | 6.70×10^{-5} | 22.5 |
| <i>SOX9</i> | 7.83×10^{-7} | 2.9 | <i>CD53</i> | 1.08×10^{-6} | 7.9 | <i>GDF5</i> | 1.50×10^{-5} | 12.2 |
| <i>FOXC2</i> | 6.43×10^{-5} | 2.7 | <i>ACVR2B</i> | 1.47×10^{-5} | 6 | <i>PDGFC</i> | 6.37×10^{-8} | 9.5 |
| <i>HOXA13</i> | 0.0476803 | 2.6 | <i>PCDHB2</i> | 2.77×10^{-6} | 5.7 | <i>FGF7</i> | 1.27×10^{-6} | 9.3 |
| <i>GLI3</i> | 0.000145827 | 2.3 | <i>ITGA4</i> | 4.67×10^{-6} | 5.7 | <i>FGF9</i> | 1.28×10^{-5} | 6.6 |
| <i>FOXA3</i> | 0.0336405 | 2.2 | <i>CD166/ALCAM</i> | 5.02×10^{-5} | 5.4 | <i>WNT5A</i> | 0.000433419 | 5.7 |
| <i>FOXP2</i> | 0.00180209 | 2.1 | <i>PTCH1</i> | 2.50×10^{-6} | 5.3 | <i>DKK3</i> | 0.000224373 | 3.7 |
| <i>HOXD11</i> | 0.0379312 | 2 | <i>PCDHB16</i> | 6.12×10^{-6} | 5.3 | <i>BMP1</i> | 3.17×10^{-7} | -3.4 |

(Continued on next page)

**Table 1. Continued**

| Prechondrocytes versus Total Limb Cells at 5–6 Weeks | | | Embryonic Prechondrocytes at 5–6 Weeks versus Immature Resting Fetal Chondrocytes at 17 Weeks | | | | | |
|--|-----------------------|-------------|---|-----------------------|-------------|--------------|-----------------------|-------------|
| Gene Symbol | p Value | Fold Change | Gene Symbol | p Value | Fold change | Gene Symbol | p Value | Fold Change |
| <i>FOXP4</i> | 1.79×10^{-5} | 1.9 | <i>PCDH9</i> | 0.000170686 | 5.2 | <i>BMP2</i> | 9.14×10^{-7} | –5.5 |
| <i>HOXD10</i> | 0.0186307 | 1.9 | <i>CD84</i> | 0.000524974 | 4.2 | <i>TGFB1</i> | 1.44×10^{-6} | –7.1 |
| <i>FOXP1</i> | 0.000117552 | 1.7 | <i>PCDH10</i> | 0.000524021 | 3.7 | <i>NGF</i> | 5.04×10^{-9} | –15.7 |
| <i>SOX8</i> | 0.00749 | 1.7 | <i>CD151</i> | 1.17×10^{-5} | –4.7 | <i>BMP6</i> | 3.56×10^{-5} | –20.7 |
| <i>GLI2</i> | 0.00126504 | 1.6 | <i>NOTCH1</i> | 2.34×10^{-8} | –4.9 | <i>TGFB2</i> | 1.01×10^{-7} | –37.2 |
| <i>GLI1</i> | 0.000173377 | 1.5 | <i>CD74</i> | 1.26×10^{-6} | –5.3 | <i>LIF</i> | 2.28×10^{-9} | –76.8 |

See also [Table S2](#).

showed that de novo chondrogenesis and condensation of mesenchymal cells is observed until 11–12 weeks ([Figure S2](#); data not shown); therefore, at 17 weeks of human development, the vast majority of chondrocytes present in articular and growth plate regions will be fully specified.

The transition of mesenchymal ancestors to highly compact, rounded chondrocytes has previously been shown to be associated with major changes in cytoskeletal composition ([Woods et al., 2007](#)). To identify specific surface antigens associated with the transition step, we compared the gene expression data of prechondrocytes (primitive cartilage-committed progenitors present only during de novo chondrogenesis) with resting periarticular chondrocytes (immature definitive chondrocytes) ([Figure 3B](#); [Table 1](#)). These data showed that the maturation of prechondrocytes into periarticular chondrocytes was associated with the progressive loss of several mesenchymal genes, including *MCAM* (encodes CD146), *NCAM1* (encodes CD56), *CD24*, *CDH2* (encodes N-cadherin) and, to a lesser extent, *ALCAM* (encodes *CD166*; [Table 1](#)). In contrast, other genes encoding surface molecules including *CD44*, *NTSE* (encodes CD73), and *SDC4* were markedly up-regulated in resting periarticular chondrocytes ([Table 1](#)). Complete lists of gene expression data are included in [Table S2](#). The expression of several key genes markedly changed in microarray analysis was confirmed by quantitative PCR ([Figure 3D](#)). IPA was then applied to identify functional groups of genes that changed during this transition; changes in cell morphology and cell movement were among the top activated categories, further indicating significant changes in cell shape in motility during chondrogenic maturation and differentiation ([Figure 3E](#)). Additionally, the microarrays identified several growth factors highly expressed in resting periarticular chondrocytes ([Table 1](#)), including transforming growth factor β 1 and 2 (*TGFB1* and 2) and leukemia inhibitory factor (*LIF*).

We next assessed the expression pattern of mesenchymal markers CD166 and CD146 in different cartilage compartments at 8 and 12 weeks of development to map cells with a prechondrocyte phenotype at more advanced stages. Similar to 5- to 6-week limbs, at 7–8 weeks of development, cells in the presumptive joint or “interzone” regions expressed CD146 ([Figure S2](#)), indicating the presence of prechondrocytes. However, by 11–12 weeks of development (and at later stages), the expression of CD146 was completely absent on the vast majority of chondrocytes, including resting periarticular chondrocytes and hypertrophic chondrocytes ([Figure S2](#)), suggesting the absence or minimal numbers of cells undergoing de novo chondrogenesis at this stage. Interestingly, despite the minimal levels of CD166 on prechondrocytes, this marker, as well as CD146, was highly expressed on the most primitive outer layer of cells in the perichondrium (another source of chondrocyte precursors) surrounding diaphyseal and metaphyseal regions of the bone rudiment. Importantly, the levels of CD166 and CD146 expression in the perichondrium markedly decreased after progenitor cell differentiation into mature chondrocytes ([Figure S2](#)).

Expression of CD146 was not exclusive to prechondrocytes. This marker was expressed at much higher levels on endothelial and perivascular cells and also on skeletal myoblasts ([Figures S3A](#) and [S3B](#)) at 6–8 weeks of development. Analysis of perivascular mesenchymal cells in situ revealed no or minimal expression of CD73 but positivity for CD166, making them phenotypically distinct from $CD73^+CD166^{low/neg}$ prechondrocytes and definitive chondrocytes ([Figure S3A](#)). The majority of skeletal myoblasts, as well as dermal fibroblasts, expressed CD166 at 5–8 weeks of development were also phenotypically distinct from chondrocytes at this stage ([Figures S3B](#) and [S3C](#)).

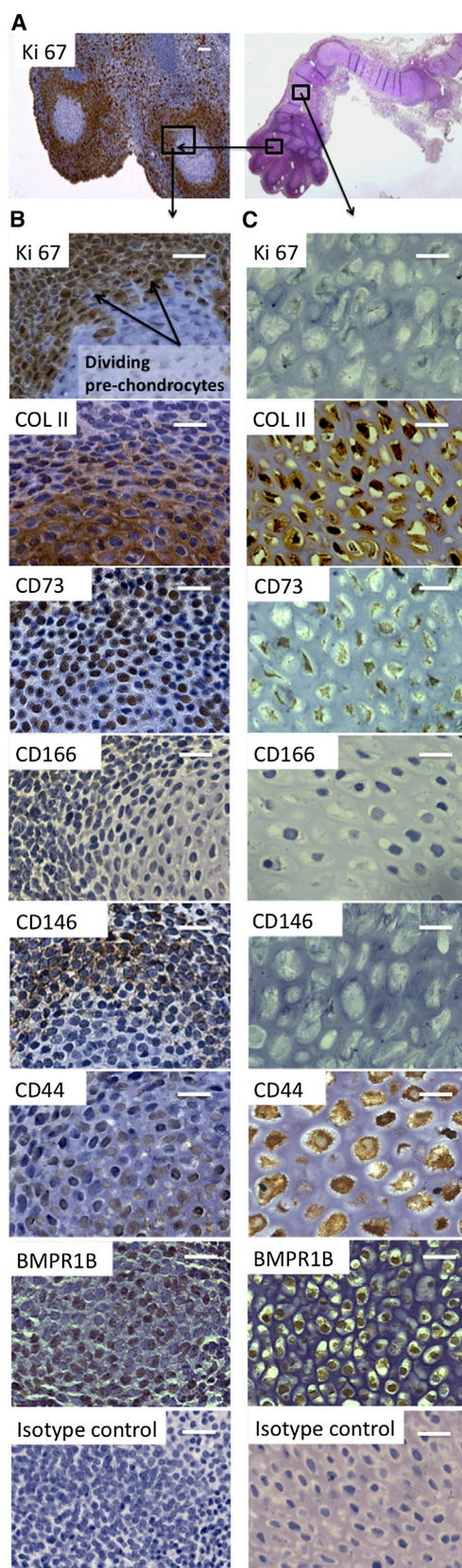


Figure 2. Prechondrocytes in Chondrogenic Condensations at 6–7 Weeks Are Proliferating and Express BMPR1B and CD146, and Are CD44^{low}/CD166^{low/neg}

(A) An overview of the upper limb at 6–7 weeks showing two focal planes assessed at high magnification.

(B and C) Immunohistochemistry for a panel of mesenchymal and chondrogenic antigens demonstrated that prechondrocytes at the periphery of condensations (B) express BMPR1B and can be distinguished from differentiated cartilage cells in the central areas of condensations and hypertrophic chondrocytes in the proximal limb region (C) via the expression of CD146, negativity for the chondrogenic matrix molecule collagen II, and low positivity for CD44 and CD166.

Positive signal is shown in brown color (3, 3'-diaminobenzidine), and nuclei were counterstained with hematoxylin. Scale bar, 20 μ m. See also Figure S1.

Finally, we assessed the expression levels of integrin alpha 5/CD49e in developing human chondrocytes. CD49e has been previously shown to mark a small cohort of cartilage progenitors located in the surface layer of adult articular cartilage (Williams et al., 2010). At 8, 12, and 17 weeks, nearly all fetal chondrocytes as well as surrounding mesenchymal cells expressed CD49e (not shown), indicating limited significance of this marker for the tracking of the chondrogenic subpopulations in early human development.

In summary, microarray and immunophenotypic analysis revealed a unique genetic signature of the most primitive human prechondrocytes and also identified a number of surface molecules and growth factors markedly up- or downregulated during prechondrocyte transition to definitive resting and more mature hypertrophic chondrocytes. In addition, these data revealed CD166 as a potentially powerful surface marker for delineating cells of the chondrogenic lineage from other mesenchymal lineages, including multipotent cell types such as the perichondrium.

Isolation of Human Primary Chondrocyte Populations by Flow Cytometry

Based on the IHC and microarray data, it was predicted that the earliest prechondrocytes are highly enriched in the CD166^{low/neg}CD73⁺ fraction of total limb cells and that the most primitive subset will also express low levels of CD146. Flow cytometric analysis of the total limb mesenchyme clearly showed the presence of a heterogeneous CD166^{low/neg}CD73⁺ subset that could be further subdivided by the level of CD146 intensity: CD146^{high} and CD146^{low/neg} (Figure 4A). From this subset, we depleted lineage-positive cells using CD45 and CD235 (glycophorin A) for the removal of hematopoietic cells, CD324/epithelial cadherin (E-CAD) to exclude keratinocytes, CD34 for the exclusion of adventitial cells, and CD31 for the exclusion of endothelial cells. CD166^{low/neg}CD146^{high}CD73⁺ cells were marked and excluded during lineage depletion,

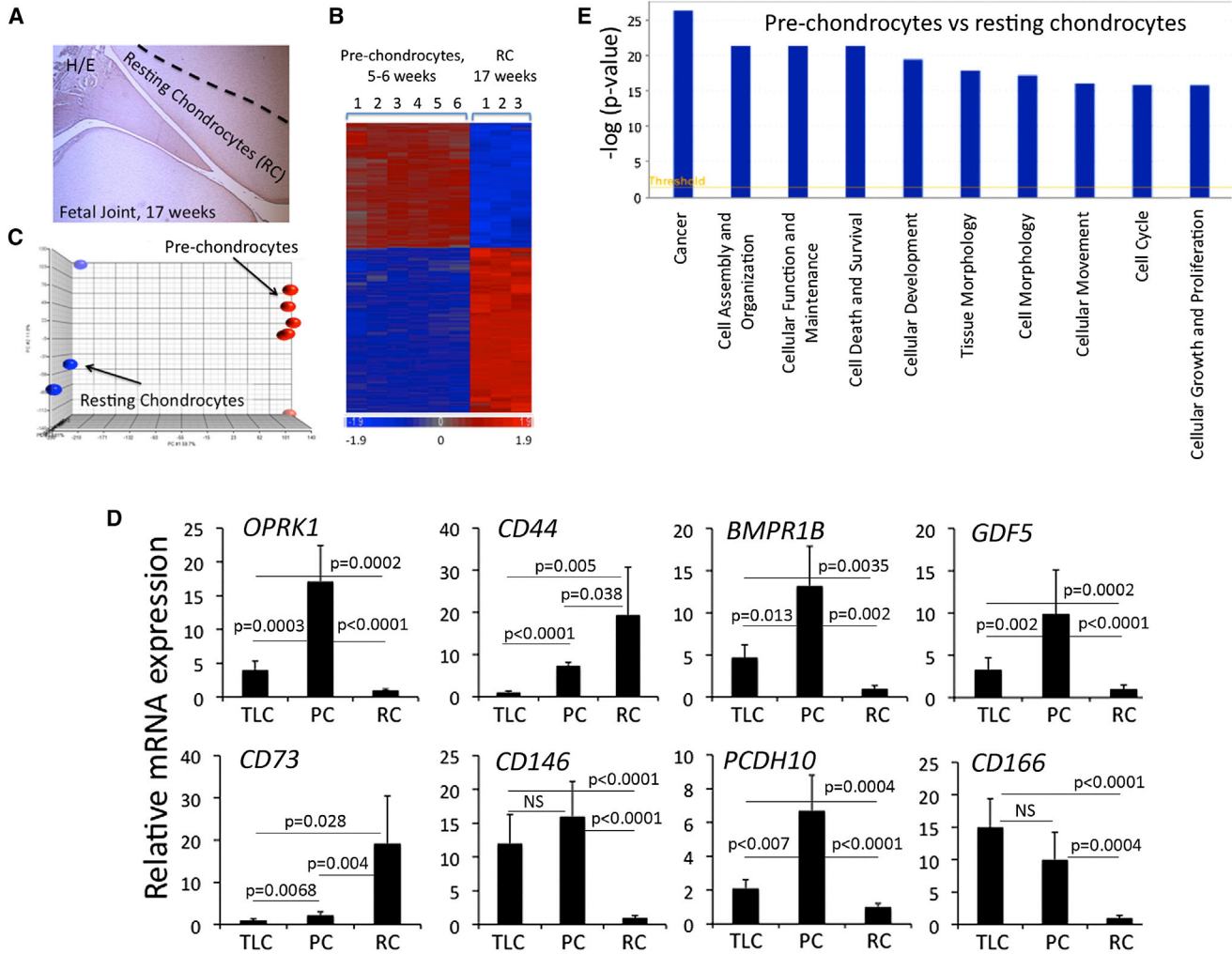


Figure 3. Prechondrocytes Are Enriched for the Expression of Mesenchymal Genes as Compared to Definitive Resting Chondrocytes (A) Resting chondrocytes were isolated by dissecting a ~200- μ m-thick layer of cells from the femoral epiphysis as indicated by the dotted line. (B) Unsupervised clustering of 1,222 genes differentially expressed between prechondrocytes (PC; six independent specimens) and definitive 17-week fetal periarticular resting chondrocytes (RC; three independent specimens).

(C) Principal component analysis performed on all probe sets demonstrated the reproducibility of data between biological replicates. (D) Expression differences of key genes enriched at specific stages of chondrocyte differentiation were validated by quantitative PCR. Expression in total limb cells (TLC) is shown for comparison. Results represent mean \pm SD; six independent specimens. NS, not statistically significant.

(E) Global functional analyses, network analyses, and canonical pathway analyses were performed using Ingenuity Pathway Analysis. The most upregulated functional groups in prechondrocytes versus definitive resting chondrocytes are shown.

See also [Figure S2](#).

indicating that they most likely represent endothelial cells positive for CD31 (data not shown). CD166^{low/neg} CD146^{low/neg}CD73⁺ cells were further subdivided into CD44^{high} and CD44^{low} subsets following the expression pattern shown for prechondrocytes and mature chondrocytes (Figures 1, 2, and 3).

To confirm that mature chondrocytes express high levels of CD44 and are CD146^{neg}, we isolated resting periarticular

chondrocytes from the proximal epiphysis of human femoral bone at 17 weeks of development. Consistent with our earlier data, no expression of CD146 or CD166 and expression of CD44 was detected on the vast majority of 17-week resting periarticular chondrocytes (Figure 4B). In 5- to 6-week limbs, the CD44^{low} subset represents 79% \pm 7.3% of CD146^{low/neg}CD166^{low/neg}CD73⁺LIN^{neg} cells while only 14.7% \pm 3.1% are mature chondrocytes expressing

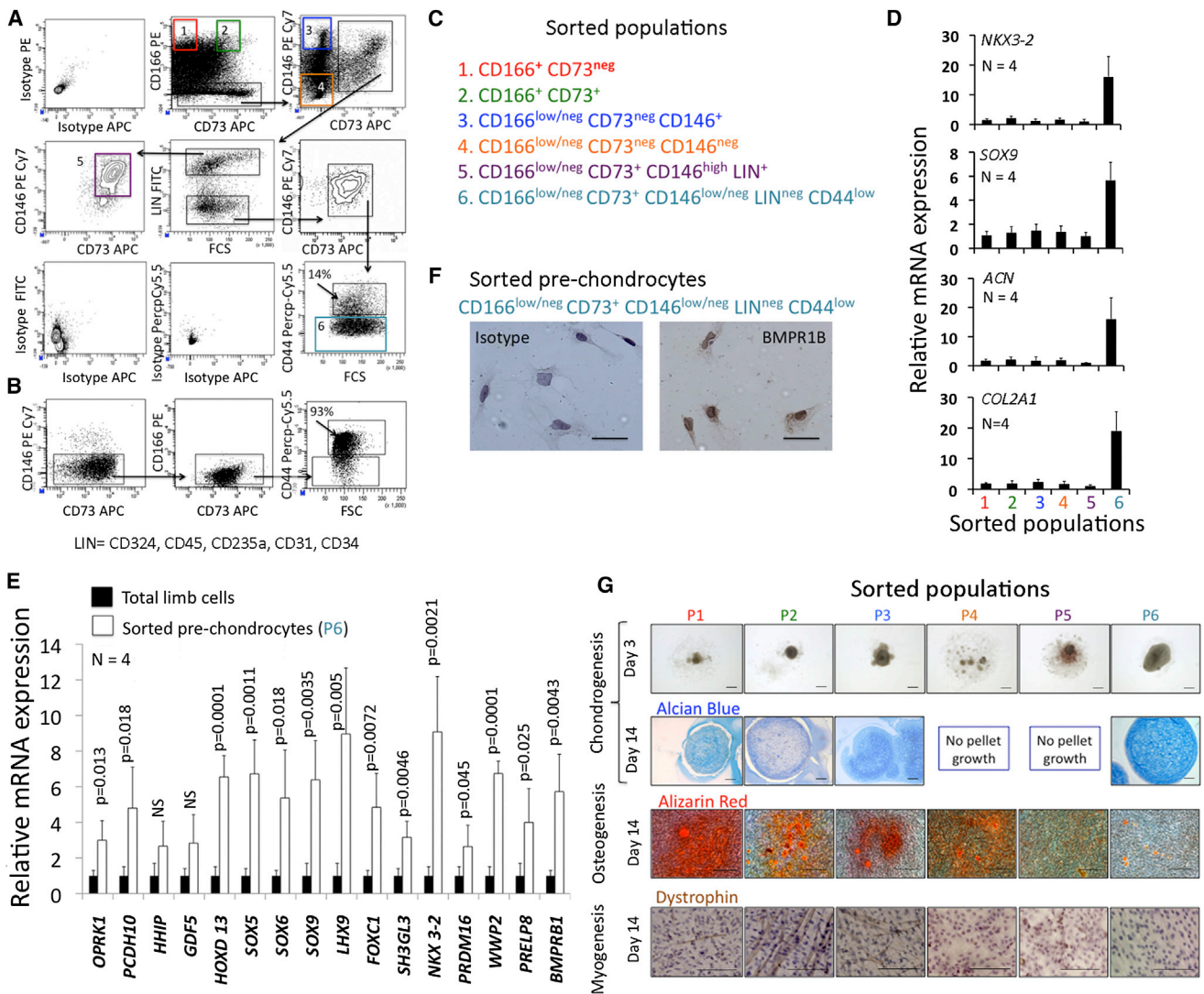


Figure 4. Prechondrocytes Can Be Prospectively Isolated from Total Limb Cells based on a CD166^{low/neg}CD73⁺CD146^{low/neg}LIN^{neg}CD44^{low} Phenotype

(A) Gating strategy used to fractionate total limb cells at 5–6 weeks of development into defined populations. The lineage cocktail used to exclude endothelial, epithelial, and hematopoietic cells (LIN) included CD324 (E-CAD), CD31, CD34, CD45, and CD235 (GLYA).

(B) Immunophenotypic profile of definitive fetal resting periarticular chondrocytes isolated at 17 weeks of development. Note the higher expression of CD44 on most cells compared to prechondrocytes.

(C and D) Gates labeled 1–6 (C) denote immunophenotypic populations isolated and tested for expression levels of the following diagnostic cartilage genes (D): *SOX9*, *NKX3-2*, *COL2A1* (collagen II), and *ACN* (aggrecan).

(E) Fluorescence-activated cell sorted CD166^{low/neg}CD73⁺CD146^{low/neg}LIN^{neg}CD44^{low} chondrogenic cells are enriched for the same genes as LCM-isolated prechondrocytes with respect to total limb cells. Mean ± SD; four independent experiments for all quantitative PCR data. NS, not statistically significant.

(F) Fluorescence-activated cell sorted CD166^{low/neg}CD146^{low/neg}CD73⁺LIN^{neg}CD44^{low} cells also express BMPR1B at the protein level. Positive staining is shown in brown (3, 3'-diaminobenzidine), and nuclei were counterstained with hematoxylin. Scale bar, 20 μM.

(G) In vitro analysis of mesenchymal lineage potential of six populations (as described in C) revealed that some populations either lacked chondrogenic potential (P4 and P5) or showed chondrogenic (Alcian blue staining), osteogenic (Alizarin red staining), and myogenic differentiation (dystrophin⁺ myotubes; brown), reflecting their initial multipotency (P1, P2, and P3). In contrast, prospective prechondrocytes (P6) uniformly generated cartilage positive for Alcian blue. Representative of three independently repeated experiments. Scale bar, 100 μm.

See also Figure S3.



high levels of CD44. In contrast, $93.3\% \pm 6.1\%$ of 17-week-old chondrocytes express high levels of CD44 (Figures 4A and 4B).

We next sorted six distinct populations identified in human 5- to 6-week-old limbs (Figure 4C) by fluorescence-activated cell sorting (FACS), isolated mRNA, and analyzed the expression of several key chondrogenic genes, including *SOX9*, *NKX3-2*, *AGN*, and *COL2A1*, in each of these populations. Quantitative PCR analysis demonstrated that $CD166^{low/neg}CD146^{low/neg}CD73^{+}CD44^{low}$ cells had the highest expression of the chondrogenic genes across the all tested populations, not including differentiated chondrocytes (Figure 4D).

To further strengthen these findings and confirm that FACS-isolated $CD166^{low/neg}CD146^{low/neg}CD73^{+}CD44^{low}$ cells represent the prechondrocytes isolated via LCM, we tested the expression levels of 16 genes found to be highly expressed in the LCM-isolated prechondrocytes in FACS-isolated $CD166^{low/neg}CD146^{low/neg}CD73^{+}CD44^{low}$ cells; total cells depleted of prechondrocytes (Figure 4E) were used as a negative control. In strong agreement with the microarray data, all tested genes were upregulated in the $CD166^{low/neg}CD146^{low/neg}CD73^{+}CD44^{low}$ population, further suggesting that this cell population represents a highly enriched pool of the earliest prechondrocytes present in chondrogenic condensations (Figure 4E). In addition, the expression of BMPR1B by sorted $CD166^{low/neg}CD146^{high}CD73^{+}CD44^{low}$ cells was confirmed by IHC (Figure 4F). However, as BMPR1B is expressed on all chondrocytes at 5–6 weeks, its significance for FACS isolation of prechondrocytes at this stage is limited.

$CD166^{low/neg}CD146^{low/neg}CD73^{+}CD44^{low}$ Cells Represent Functional Human Chondrocyte Progenitors

Next, we carried out in vitro functional studies to confirm the chondrogenic potential and commitment of $CD166^{low/neg}CD146^{low/neg}CD73^{+}CD44^{low}$ cells as well as the other five populations sorted from the same limb samples (Figure 4C). In vitro pellet assays, designed to test mesenchymal lineage potential, performed on $CD166^{low/neg}CD146^{low/neg}CD73^{+}CD44^{low}$ (population 6) cells isolated from 5- to 6-week limbs confirmed their predominate chondrogenic potential (Figure 4G), while other populations had either no chondrogenic potential (populations 4 and 5) or limited ability to form cartilage tissue (populations 1 and 2). Populations 1, 2, and 3 also showed very prominent osteogenic potential, indicating the presence of multipotent cells or/and multiple lineage-committed progenitors in these fractions (Figure 4G). Myogenic potential (formation of myofibers) was especially prominent in population 2. These data confirmed the predominate chondrogenic potential of $CD166^{low/neg}CD146^{low/neg}CD73^{+}CD44^{low}$ cells and

further highlighted the utility of CD166 as a marker for cells with potential to generate other mesenchymal lineages.

BMPR1B and LIFR Are Restricted to Resting Chondrocytes at Later Developmental Stages

Immunohistochemistry showed that BMPR1B is expressed on prechondrocytes at 5–6 weeks of development (Table 1; Figure 4F) and also more broadly on more mature chondrocytes in the center of chondrogenic condensations at 6–7 weeks (Figure 2C). Starting in 8-week limbs and progressing through gestation, BMPR1B is expressed primarily on resting chondrocytes in the surface layers of articular cartilage; more differentiated chondrocytes located in deeper zones did not express BMPR1B (Figure 5A). Interestingly, a similar pattern of expression for LIFR was also observed, while both resting periarticular chondrocytes and adjacent synovial cells expressed the ligand LIF (Figure 5B). In postnatal articular cartilage (Figure 5C), $BMPR1B^{+}$ and $LIFR^{+}$ cells were also clearly detectable in the superficial zone coinciding with the known location of the most primitive cartilage progenitor pool (Dowthwaite et al., 2004), but not in the more differentiated deep zone. Of note, not all $BMPR1B^{+}$ cells expressed LIFR. In postnatal growth plates, where chondrogenesis is still active, immature chondrogenic cells were also $BMPR1B^{+}$ and $LIFR^{+}$, while differentiated chondrocytes were negative for both (Figure 5D). Finally, BMPR1B and LIFR are preferentially expressed on cells located in the superficial zone versus chondrocytes present in the deep zone in articular cartilage from a knee joint even at 60 years of age (Figure 5E). Similar to fetal joints, synovial cells in older adult joints express LIF (Figure 5F). To further confirm that BMPR1B is enriched on less differentiated chondrocytes after de novo chondrogenesis is completed (after 12 weeks of development), we isolated $BMPR1B^{+}$ and $BMPR1B^{-}$ chondrocytes from 17-week fetal limb specimens by flow cytometry and compared the expression levels of the immature chondrocyte gene *SOX9* and highly specific hypertrophic marker *COL10A1* in both sorted populations (Figure 5G). $BMPR1B^{+}$ chondrocytes expressed 10-fold-higher levels of *SOX9* but had much lower levels of *COL10A1*. Together, these data implicate BMPR1B and LIFR as potential surface markers for immature chondrocytes after the culmination of de novo chondrogenesis and throughout the human lifespan.

The Generation and Maintenance of Prechondrocytes from PSC-Derived Mesenchyme Is Marked by the Progressive Loss of CD166 Expression and Acquisition of BMPR1B

We next wanted to determine if the surface markers identified during human development could be applied to the generation of chondrocytes from human PSCs. Our group has recently described a multipotent embryonic

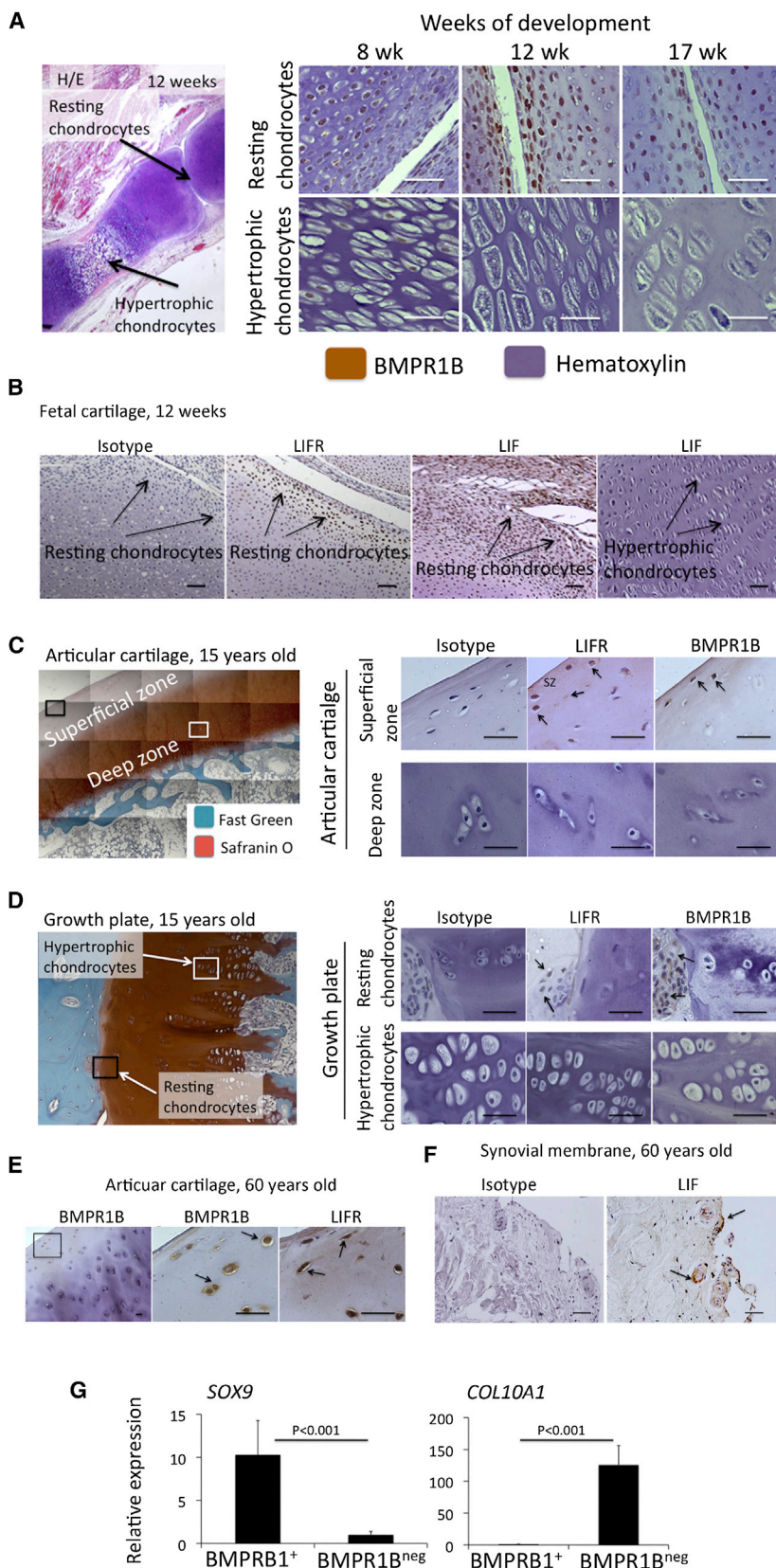


Figure 5. BMPR1B and LIFR Delineate Resting Chondrocytes after De Novo Chondrogenesis

(A) Developmental dynamics of BMPR1B expression in human chondrocytes. BMPR1B is highly expressed in resting periarticular chondrocytes at 8, 12, and 17 weeks of development but is clearly absent in hypertrophic chondrocytes after 12 weeks. Positive signal is shown in brown color (3, 3'-diaminobenzidine), and nuclei were counterstained with hematoxylin (blue).

(B) LIFR is expressed by resting chondrocytes in the periarticular region and not by hypertrophic chondrocytes, while LIF is expressed by both resting chondrocytes and neighboring synovial cells.

(C) In postnatal articular cartilage, resting chondrocytes in the superficial zone (negative for Safranin O and fast green staining) express both BMPR1B and LIFR, while hypertrophic chondrocytes in the deep zone (positive for Safranin O) are negative for both proteins.

(D) Reserve chondrocytes in the growth plate region at the same stage also express BMPR1B and LIFR; hypertrophic chondrocytes are negative.

(E and F) At later adult stages, a subset of BMPR1B⁺ and LIFR⁺ cells (E, arrows) remain in the surface layer of normal articular cartilage from the knee joint, while LIF (F) is secreted by synovial cells. In all panels, positive staining is shown in brown (3, 3'-diaminobenzidine); nuclei were counterstained with hematoxylin. Scale bar, 50 μm.

(G) BMPR1B⁺ cells isolated using FACS from 17-week periarticular regions evidence enrichment for the chondrocyte progenitor gene *SOX9*, but express much lower levels of the hypertrophic gene *COL10A1* with respect to BMPR1B^{neg} cells isolated from the same region. Mean ± SD; four independent experiments.

See also Figure S4.



mesodermal progenitor (EMP) isolated from PSCs based on expression of surface markers of epithelial-to-mesenchymal transition (Evseenko et al., 2010). Our previous studies showed that the EMP population gives rise to lineage-restricted hematoendothelial, cardiovascular, and mesenchymal progenitors (functionally resembling embryonic myogenic, osteogenic, and chondrogenic mesenchyme). The earliest skeletogenic mesenchymal cells were identified by high levels of CD166, CD146, and PDGFR α expression and lacked expression of CD326, CD34, and KDR (Evseenko et al., 2010). The earliest mesenchymal cells expressed no or minimal levels of BMPR1B. Although PSC-derived mesenchymal progenitors could be differentiated into osteogenic, myogenic, adipogenic, and chondrogenic cells, the onset of chondrogenic differentiation and immunophenotypes of emerging chondrocytes and transition to hypertrophic chondrocytes was not defined.

We hypothesized that the previously described multipotent mesenchymal population generated from human PSCs during mesodermal differentiation was analogous to mesenchymal progenitors found in limb rudiments prior to the onset of chondrogenesis. We further predicted, based on our developmental studies, that chondrogenic differentiation of these cells could be tracked by the downregulation of CD166 and the acquisition of BMPR1B by cells resembling primary prechondrocytes/resting chondrocytes while hypertrophic chondrocytes generated from PSC were expected to be BMPR1B^{neg}. To test this hypothesis, PSC-derived mesenchymal cells were plated into micromass high-density culture to mimic chondrogenic condensation (Figure 6A) in the presence of chondrogenesis-inducing factors Sonic Hedgehog (SHH) and BMP4 as well as pro-survival factors FGF2 and IGF1 in serum free conditions. The chondrogenic effects of SHH at the progenitor stage have been well documented (Murtaugh et al., 1999; Zeng et al., 2002). In the current study, the SHH receptor Patched 1 (*PTCH 1*) was found to be on the list of the most upregulated genes in prechondrocytes at 5–6 weeks of development (Table 1), and its expression was also confirmed on PSCs and PSC-derived mesenchyme (not shown).

Based on our microarray data and published literature, we hypothesized that transforming growth factor β (TGF- β) and LIF signaling may induce committed chondrocytes to remain in an undifferentiated state (Table 1), while BMP signaling may promote hypertrophy. Several BMP superfamily members including BMP2, BMP4, and BMP7 as well as GDF5 have previously been shown to induce chondrogenesis in vivo and in vitro, and prolonged exposure to these factors is known to drive chondrocyte maturation and hypertrophy (Coleman et al., 2013; Zhang et al., 2003; Bandyopadhyay et al., 2006; Coleman and Tuan, 2003; Grimsrud et al., 1998). To test this hypothesis in our system, we cultured human primary fetal chondrocytes

with various cytokines (Figure S4). BMP4 and BMP7 had the most prominent stimulatory effect on *COL10A1* gene expression in validation studies, indicative of the adoption of a hypertrophic phenotype; inclusion of TGF- β 1 and LIF individually had a small effect, but the combination of the two significantly prevented the induction of *COL10A1* expression during culture.

We then applied these conditions to PSC-derived cells. Generated aggregates were cultured for 5, 10, and 15 days and then analyzed for chondrogenic characteristics (Figures 6B–6D). To further dissect the molecular profile of cultured cells, we dissociated aggregates for FACS analysis at days 5, 10, and 15 of culture. At day 10, BMPR1B showed the highest level of expression; this surface molecule was expressed on 60%–70% of cells cultured in the presence of LIF and TGF- β 1, while levels of CD166 were downregulated, suggesting that the majority of mesenchymal cells transitioned into phenotypic prechondrocyte/resting (immature) chondrocyte (Figure 6B). In contrast, only 2%–4% of cells cultured in the presence of BMP7 were BMPR1B⁺, consistent with the low levels of expression of this receptor on hypertrophic chondrocytes (Figure 6B). Quantitative PCR analysis revealed significantly higher levels of the chondrocyte maturation-associated genes *MTN1*, *RUNX2*, and *COL10A1* in aggregates cultured in the presence of BMP7, while genes whose expression is enriched in superficial zone of articular cartilage where resting chondrocytes are located (*BMPR1B*, *PRG4*, and *SOX9*) were elevated in BMPR1B⁺CD166^{low/neg} cells isolated from aggregates cultured in the presence of TGF- β 1 and LIF (Figure S5A). PCR analysis confirmed progressive downregulation of BMPR1B gene expression, initially expressed on aggregated mesenchymal cells at the time of chondrogenic induction, in cultures exposed to BMP7 for more than 10 days (Figure S5B). In both cultures, most cells expressed CD73 and CD44, indicating limited significance of these markers for the tracking of chondrogenic cells generated from PSCs (not shown).

We next determined the quantitative expression levels of chondrogenic genes in three distinct populations isolated from aggregates cultured in the presence of TGF- β 1 and LIF by FACS: (1) CD166⁺BMPR1B^{low/neg}, (2) CD166^{low/neg}BMPR1B⁺, and (3) CD166^{low/neg}BMPR1B^{low/neg} cells. Quantitative PCR analysis showed that only CD166^{low/neg}BMPR1B⁺ cells expressed both progenitor/interzone genes (*SOX9* and *GDF5*) as well as *COL2A1*, while minimal levels of hypertrophic chondrocyte marker *COL10A1* were detected. CD166⁺BMPR1B^{low/neg} cells showed minimal expression of chondrogenic genes, while CD166^{low/neg}BMPR1B^{low/neg} evidenced an expression profile more typical for chondrocytes undergoing terminal differentiation and hypertrophy (Figure 6C), indicating that this population is enriched for terminally differentiated chondrocytes.

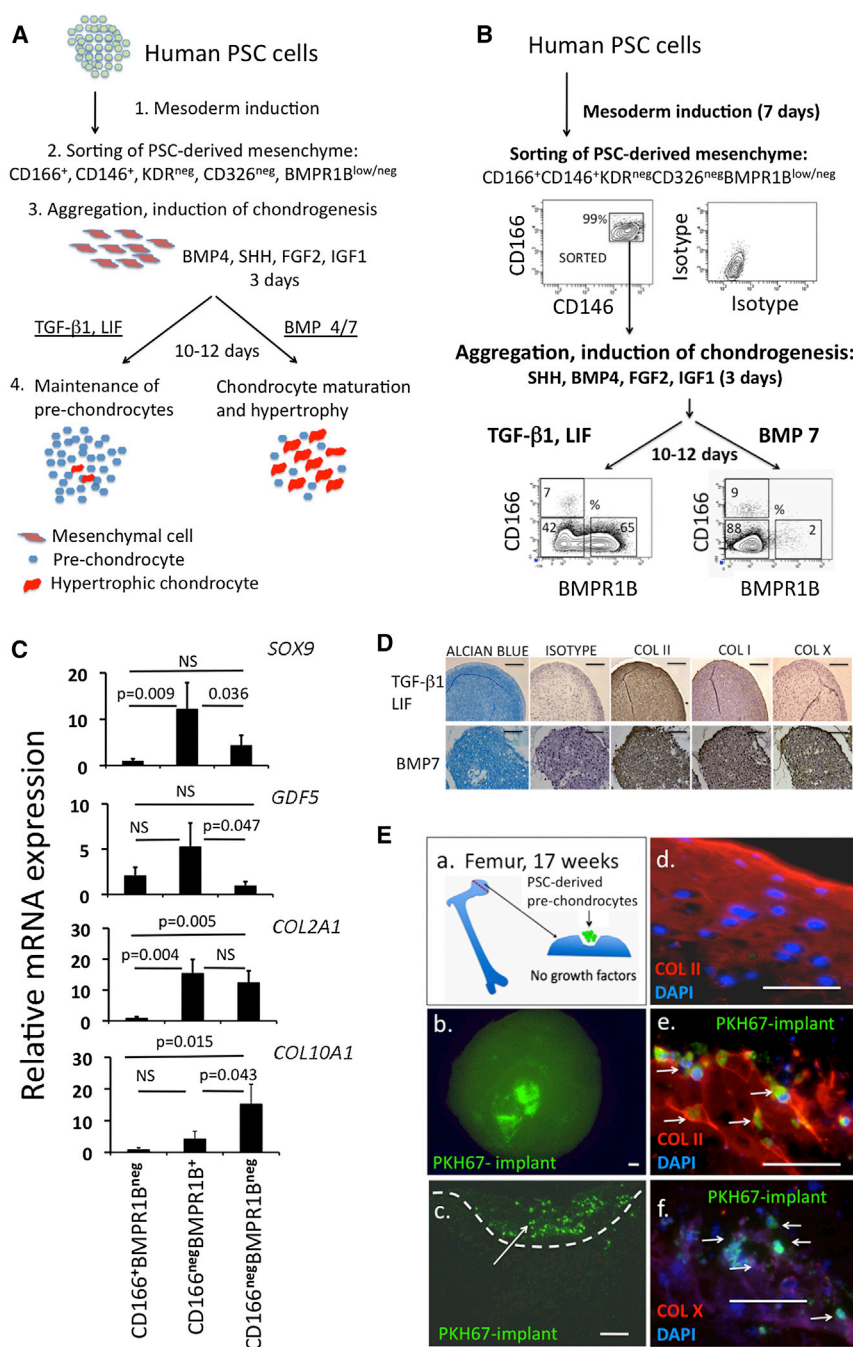


Figure 6. Emerging PSC-Derived Chondrocytes Can Be Enriched Using a Similar Strategy Defined by Chondrocyte Ontogeny in Vivo

(A) Experimental scheme depicting the generation of PSC-derived chondrocytes following the induction of mesenchyme differentiation.

(B) Immunophenotypic profiles used to isolate prechondrocyte-like and mature chondrocytes generated from PSC-derived mesenchyme after chondrogenic aggregation.

(C) Expression of chondrogenic genes in CD166^{low/neg}BMPR1B^{neg}, CD166^{low/neg}BMPR1B⁺, and CD166⁺BMPR1B^{neg} cells isolated from chondrogenic aggregates cultured in the presence of LIF and TGF-β1. CD166^{low/neg}BMPR1B⁺ cells expressed higher levels of prechondrocyte genes compared to the other two populations and showed significantly lower expression levels of COL10A1 than CD166^{low/neg}BMPR1B^{neg} cells (mean ± SD; three independent experiments); NS, not statistically significant.

(D) Chondrogenesis-committed mesenchymal cells cultured in the presence of TGF-β1 and LIF (top row) generate cartilage matrix positive for Alcian blue and collagen II, with minimal levels of collagen I and X, while mesenchymal cell aggregates cultured in the presence of BMP7 show hypertrophic morphology and deposit high levels of collagen X (bottom row). Scale bar shown for images is 100 μm.

(E) a. PSC-derived CD166^{low/neg}BMPR1B⁺ cells were isolated by FACS, labeled with PKH67 green, and deposited into explants from fetal hip joints. b. Explant viewed from above at the time of harvest showing persistence of PKH67-labeled cells after 14 days. c. Transverse section through the explant. d. Uniform Collagen II staining of chondrocytes in the uninjured surface of the explant. e. PSC-derived prechondrocyte-like cells integrate into the injured region and produce collagen II, but not collagen X (f). Scale bar, 50 μm. See also Figure S5.

Immunohistochemical analysis of aggregates at day 15 showed significant levels of collagen II and glycosaminoglycans present in all aggregates, confirming that all cultures were undergoing chondrogenesis (Figure 6D). However, cells cultured in the presence of BMP7 had hypertrophic morphology and deposited significantly higher levels of collagen X (Figure 6D). We next tested the multilineage potential of the CD166^{low/neg}BMPR1B⁺ cells. In contrast to multipotent mesenchymal cells derived from PSCs

described in our previous studies (Evseenko et al., 2010), this population showed no or minimal osteogenic, adipogenic, and myogenic potential (Figure S5C). Finally, sorted and PKH67-labeled (green) CD166^{low/neg}BMPR1B⁺ were implanted into the surface layer of femoral cartilaginous epiphysis dissected from fetal 17-week specimens and cultured. Immunofluorescent analysis performed 14 days later showed clear integration of PSC-derived cells into the existing cartilage tissue, robust deposition of collagen II,



and lack of the hypertrophic marker collagen X in the matrix surrounding implanted cells (Figure 6E). Overall, these experiments revealed that $CD166^{low/neg}BMPR1B^+$ cells derived from PSCs represent cartilage-committed cells with a molecular and functional profile similar to undifferentiated prechondrocytes/resting chondrocytes present during human development and that LIF and TGF- β signaling can be used to promote a nonhypertrophic state in these cells.

DISCUSSION

In summary, we have used LCM and FACS to isolate and characterize for the first time the earliest cartilage-committed and structurally distinct prechondrocytes and definitive chondrocytes during early human embryogenesis. Using immunophenotypic markers, gene expression, and functionality, we showed that a developmental paradigm allows for the generation and enrichment of prechondrocytes/immature chondrocytes during PSC differentiation based on the expression patterns of BMPR1B and CD166 and signaling pathways important during development. Altogether, these data detail a potential approach for the generation of functional definitive human chondrocytes from PSCs that may drive new methodologies for cartilage tissue engineering.

We first identified surface markers that distinguish the earliest prechondrocytes from nonchondrogenic cell types; subsequent comparison of prechondrocytes with differentiated, definitive resting (immature) chondrocytes located in the superficial periarticular regions within fetal joints led to the identification of a combination of surface markers enriched on both cell types and demarcating them from chondrocytes undergoing maturation and hypertrophy. The expression of CD166 and CD146 has been previously reported to mark highly invasive and migratory mesenchymal cells in normal and pathological conditions (Swart, 2002; Swart et al., 2005; Zeng et al., 2012). Moreover, CD146 has been shown to be directly involved in the process of epithelial-to-mesenchymal transition through the positive regulation of Slug (Zeng et al., 2012). In good agreement with these studies, loss of the mesenchymal phenotype and transition of cartilage-committed mesenchymal cells or prechondrocytes to differentiated nonmotile chondrocytes is associated with the progressive loss of CD166 of CD146.

A combination of TGF- β 1 and LIF was used in this study to inhibit excessive cartilage maturation and hypertrophy and favor the generation and persistence of primary and PSC-derived cartilage progenitors. Although the antidifferentiation properties of LIF have been well documented in the fields of pluripotent stem cells, hematopoiesis, and neurobiology (Audet et al., 2001; Bonaguidi et al., 2005;

Smith et al., 1988), their role in the regulation of chondrogenesis is completely novel. Synovial cells of both fetal and adult normal joints highly express LIF (Figure 5), indicating that this factor may be implicated in the maintenance of the most primitive progenitors located in the superficial layer of articular cartilage. Indeed, LIFR was primarily localized in resting chondrocytes also positive for BMPR1B, while LIF and TGF- β 1 and TGF- β 2 were among the top molecules enriched in definitive resting chondrocytes (Table 1). Moreover, our validation studies on fetal chondrocytes suggest that these factors may prevent chondrocyte maturation and hypertrophy. More studies are needed to characterize BMPR1B⁺ cells in adult joints and fully define the role of LIF in the regulation of these cells. Our data suggest that utilizing the LIF signaling axis may further advance engineering of functionally superior cartilage implants for joint surface repair in patients with cartilage injury or arthritis.

In summary, we have for the first time characterized the earliest stages of human chondrogenic development. Starting with the distinct morphological identity of prechondrocytes, we found a unique combination of surface markers ($CD166^{low/neg}CD146^{low/neg}CD73^+CD44^{low}BMPR1B^+$) that distinguishes these cells from other populations in the developing limb and directs the enrichment of chondrogenic progenitors. Subsequent comparison of the gene expression profile of prechondrocytes with resting periarticular chondrocytes, in conjunction with immunohistochemical analysis, led to the identification of the LIF, TGF- β , and BMP signaling pathways as potential regulators of the differentiation state of chondrocytes. Application of these findings permitted the generation of functional immature chondrocyte cells from pluripotent stem cells. The identification of specific phenotypic signatures for primitive prechondrocytes and definitive resting chondrocytes will now permit further delineation of the molecular regulation of chondrogenic commitment, growth plate versus articular cartilage fate choice, and hypertrophy in humans. It may also contribute to understanding of how these processes are affected during aberrant chondrogenesis in disease states. Finally, characterization of the earliest primary chondrocytes provides essential knowledge for the generation of purified cartilage cells from PSCs and represents a unique target for cartilage tissue engineering.

EXPERIMENTAL PROCEDURES

Human fetal tissues were obtained from Novogenix Laboratories following informed consent and elective termination. Developmental age was determined by ultrasound. Adult articular chondrocytes and synovial membrane were obtained from National Disease Research Interchange. Postnatal, healthy,



paraffin-embedded joint and growth plate specimens (N = 3) were kindly donated by Dr Marcel Karperien from the University of Twente (Netherlands). All donated material was anonymous and carried no personal identifiers. Differentiation potential of PSCs was studied using the H1 cell line (Madison, WI) or fully validated lines UCLA3 or HIPS23 derived at the University of California, Los Angeles (Los Angeles, CA). Fetal specimens, adult specimens, and/or PSC-derived lineages were analyzed using LCM, flow cytometry, microarray analysis, PCR, and immunohistochemistry as well as chondrogenic, myogenic, adipogenic, and osteogenic assays. Detailed description of all methods and statistical tests used for analyses of data is available in the [Supplemental Experimental Procedures](#).

ACCESSION NUMBERS

The NCBI Gene Expression Omnibus accession number for microarray data reported in this study is GSE51812.

SUPPLEMENTAL INFORMATION

Supplemental Information includes Supplemental Experimental Procedures, five figures, and two tables and can be found with this article online at <http://dx.doi.org/10.1016/j.stemcr.2013.10.012>.

ACKNOWLEDGMENTS

The authors thank Dr. Marcel Karperien from the University of Twente, Netherlands for providing growth plate and articular cartilage specimens. The authors are also grateful to Ms. Felicia Codrea and Ms. Jessica Scholes from UCLA FACS Core for their help with sample analysis and sorting. This work is supported by National Institutes of Health grant K01AR061415, DOD grant OR120161, and ANRF research grant and CIRM RB3-05217 grant.

Received: June 16, 2013

Revised: October 18, 2013

Accepted: October 30, 2013

Published: December 12, 2013

REFERENCES

Andersson, G., Bouchard, J., Bozic, K., Campbell, R., Cisternas, M., Correa, A., Cosman, E., and Cragan, J. (2011). The Burden of Musculoskeletal Diseases in the United States (Rosemont, IL: The American Academy of Orthopaedic Surgeons).

Audet, J., Miller, C.L., Rose-John, S., Piret, J.M., and Eaves, C.J. (2001). Distinct role of gp130 activation in promoting self-renewal divisions by mitogenically stimulated murine hematopoietic stem cells. *Proc. Natl. Acad. Sci. USA* *98*, 1757–1762.

Bandyopadhyay, A., Tsuji, K., Cox, K., Harfe, B.D., Rosen, V., and Tabin, C.J. (2006). Genetic analysis of the roles of BMP2, BMP4, and BMP7 in limb patterning and skeletogenesis. *PLoS Genet.* *2*, e216.

Baur, S.T., Mai, J.J., and Dymecki, S.M. (2000). Combinatorial signaling through BMP receptor IB and GDF5: shaping of the distal

mouse limb and the genetics of distal limb diversity. *Development* *127*, 605–619.

Bonaguidi, M.A., McGuire, T., Hu, M., Kan, L., Samanta, J., and Kessler, J.A. (2005). LIF and BMP signaling generate separate and discrete types of GFAP-expressing cells. *Development* *132*, 5503–5514.

Buckwalter, J.A., and Mankin, H.J. (1998). Articular cartilage repair and transplantation. *Arthritis Rheum.* *41*, 1331–1342.

Cameron, T.L., Belluoccio, D., Farlie, P.G., Brachvogel, B., and Bate-man, J.F. (2009). Global comparative transcriptome analysis of cartilage formation in vivo. *BMC Dev. Biol.* *9*, 20.

Coleman, C.M., and Tuan, R.S. (2003). Growth/differentiation factor 5 enhances chondrocyte maturation. *Dev. Dyn.* *228*, 208–216.

Coleman, C.M., Vaughan, E.E., Browe, D.C., Mooney, E., Howard, L., and Barry, F. (2013). Growth differentiation factor-5 enhances in vitro mesenchymal stromal cell chondrogenesis and hypertrophy. *Stem Cells Dev.* *22*, 1968–1976.

DeLise, A.M., Fischer, L., and Tuan, R.S. (2000). Cellular interactions and signaling in cartilage development. *Osteoarthritis Cartilage* *8*, 309–334.

Dowthwaite, G.P., Bishop, J.C., Redman, S.N., Khan, I.M., Rooney, P., Evans, D.J., Haughton, L., Bayram, Z., Boyer, S., Thomson, B., et al. (2004). The surface of articular cartilage contains a progenitor cell population. *J. Cell Sci.* *117*, 889–897.

Evseenko, D., Zhu, Y., Schenke-Layland, K., Kuo, J., Latour, B., Ge, S., Scholes, J., Dravid, G., Li, X., MacLellan, W.R., and Crooks, G.M. (2010). Mapping the first stages of mesoderm commitment during differentiation of human embryonic stem cells. *Proc. Natl. Acad. Sci. USA* *107*, 13742–13747.

Gelse, K., Mühle, C., Franke, O., Park, J., Jehle, M., Durst, K., Göken, M., Hennig, F., von der Mark, K., and Schneider, H. (2008). Cell-based resurfacing of large cartilage defects: long-term evaluation of grafts from autologous transgene-activated periosteal cells in a porcine model of osteoarthritis. *Arthritis Rheum.* *58*, 475–488.

Goldring, M.B., Tsuchimochi, K., and Ijiri, K. (2006). The control of chondrogenesis. *J. Cell. Biochem.* *97*, 33–44.

Grimrud, C.D., Rosier, R.N., Puzas, J.E., Reynolds, P.R., Reynolds, S.D., Hicks, D.G., and O'Keefe, R.J. (1998). Bone morphogenetic protein-7 in growth-plate chondrocytes: regulation by retinoic acid is dependent on the stage of chondrocyte maturation. *J. Orthop. Res.* *16*, 247–255.

Hall, B.K., and Miyake, T. (1995). Divide, accumulate, differentiate: cell condensation in skeletal development revisited. *Int. J. Dev. Biol.* *39*, 881–893.

Koyama, E., Shibukawa, Y., Nagayama, M., Sugito, H., Young, B., Yuasa, T., Okabe, T., Ochiai, T., Kamiya, N., Rountree, R.B., et al. (2008). A distinct cohort of progenitor cells participates in synovial joint and articular cartilage formation during mouse limb skeletogenesis. *Dev. Biol.* *316*, 62–73.

Murtaugh, L.C., Chyung, J.H., and Lassar, A.B. (1999). Sonic hedgehog promotes somitic chondrogenesis by altering the cellular response to BMP signaling. *Genes Dev.* *13*, 225–237.

Nakayama, N., Duryea, D., Manoukian, R., Chow, G., and Han, C.Y. (2003). Macroscopic cartilage formation with embryonic



- stem-cell-derived mesodermal progenitor cells. *J. Cell Sci.* *116*, 2015–2028.
- Oldershaw, R.A., Baxter, M.A., Lowe, E.T., Bates, N., Grady, L.M., Soncin, F., Brison, D.R., Hardingham, T.E., and Kimber, S.J. (2010). Directed differentiation of human embryonic stem cells toward chondrocytes. *Nat. Biotechnol.* *28*, 1187–1194.
- Provot, S., and Schipani, E. (2005). Molecular mechanisms of endochondral bone development. *Biochem. Biophys. Res. Commun.* *328*, 658–665.
- Smith, A.G., Heath, J.K., Donaldson, D.D., Wong, G.G., Moreau, J., Stahl, M., and Rogers, D. (1988). Inhibition of pluripotential embryonic stem cell differentiation by purified polypeptides. *Nature* *336*, 688–690.
- Swart, G.W. (2002). Activated leukocyte cell adhesion molecule (CD166/ALCAM): developmental and mechanistic aspects of cell clustering and cell migration. *Eur. J. Cell Biol.* *81*, 313–321.
- Swart, G.W., Lunter, P.C., Kilsdonk, J.W., and Kempen, L.C. (2005). Activated leukocyte cell adhesion molecule (ALCAM/CD166): signaling at the divide of melanoma cell clustering and cell migration? *Cancer Metastasis Rev.* *24*, 223–236.
- Toh, W.S., Guo, X.M., Choo, A.B., Lu, K., Lee, E.H., and Cao, T. (2009). Differentiation and enrichment of expandable chondrogenic cells from human embryonic stem cells in vitro. *J. Cell. Mol. Med.* *13* (9B), 3570–3590.
- Umeda, K., Zhao, J., Simmons, P., Stanley, E., Elefanty, A., and Nakayama, N. (2012). Human chondrogenic paraxial mesoderm, directed specification and prospective isolation from pluripotent stem cells. *Sci. Rep.* *2*, 455.
- van Osch, G.J., Brittberg, M., Dennis, J.E., Bastiaansen-Jenniskens, Y.M., Erben, R.G., Konttinen, Y.T., and Luyten, F.P. (2009). Cartilage repair: past and future—lessons for regenerative medicine. *J. Cell. Mol. Med.* *13*, 792–810.
- Williams, R., Khan, I.M., Richardson, K., Nelson, L., McCarthy, H.E., Analbelsi, T., Singhrao, S.K., Dowthwaite, G.P., Jones, R.E., Baird, D.M., et al. (2010). Identification and clonal characterisation of a progenitor cell sub-population in normal human articular cartilage. *PLoS ONE* *5*, e13246.
- Woods, A., Wang, G., and Beier, F. (2007). Regulation of chondrocyte differentiation by the actin cytoskeleton and adhesive interactions. *J. Cell. Physiol.* *213*, 1–8.
- Yamashita, A., Nishikawa, S., and Rancourt, D.E. (2010). Identification of five developmental processes during chondrogenic differentiation of embryonic stem cells. *PLoS ONE* *5*, e10998.
- Zeng, L., Kempf, H., Murtaugh, L.C., Sato, M.E., and Lassar, A.B. (2002). Shh establishes an Nkx3.2/Sox9 autoregulatory loop that is maintained by BMP signals to induce somitic chondrogenesis. *Genes Dev.* *16*, 1990–2005.
- Zeng, Q., Li, W., Lu, D., Wu, Z., Duan, H., Luo, Y., Feng, J., Yang, D., Fu, L., and Yan, X. (2012). CD146, an epithelial-mesenchymal transition inducer, is associated with triple-negative breast cancer. *Proc. Natl. Acad. Sci. USA* *109*, 1127–1132.
- Zhang, D., Schwarz, E.M., Rosier, R.N., Zuscik, M.J., Puzas, J.E., and O’Keefe, R.J. (2003). ALK2 functions as a BMP type I receptor and induces Indian hedgehog in chondrocytes during skeletal development. *J. Bone Miner. Res.* *18*, 1593–1604.